

Machine Learning Based Top Quark and W Jet Tagging to Hadronic Four-Top Final States Induced by SM as well as BSM Processes

Jiří Kvita¹, Petr Baron^{1*}, Monika Machalová², Radek Přívara¹, Rostislav Vodák^{2†}, Jan Tomeček²

¹ Joint Laboratory of Optics of Palacký University Olomouc and Institute of Physics of Czech Academy of Sciences, Czech Republic

² Department of Mathematical Analysis and Applications of Mathematics, Palacký University Olomouc, Czech Republic

★ petr.baron@upol.cz, † rostislav.vodak@upol.cz



*The 17th International Workshop on
Top Quark Physics (TOP2024)
Saint-Malo, France, 22-27 September 2024
doi:10.21468/SciPostPhysProc.?*

Abstract

We study the application of selected ML techniques to the recognition of a substructure of hadronic final states (jets) and their tagging based on their possible origin in current HEP experiments using simulated events and a parameterized detector simulation. The results are then compared with the cut-based method.

Copyright attribution to authors.

This work is a submission to SciPost Phys. Proc.

License information to appear upon publication.

Publication information to appear upon publication.

Received Date

Accepted Date

Published Date

1 Introduction

Jets as hadronic final states are an inevitable consequence of the quantum chromodynamics (QCD) [1], the force between strongly interacting matter constituents of quarks and gluons. In hadron collisions, jets are important final states and signatures of objects of high transverse momentum. In cases of large jet transverse momenta, i.e. with a larger Lorentz boost in the plane perpendicular to the proton beam, decay products of hadronically decaying W bosons or top quarks are collimated so that they form one large boosted jet in the detector. This study aims to perform jet tagging for top quarks and W bosons using a machine learning (ML) approach and compare the results with a traditional cut-based method.

2 Data Samples

Five datasets were generated using the MadGraph5 with different transverse momentum selection criteria on the jets and mass of hypothetical Z' particle which decays into top quarks.

Subsequently two new datasets were derived by unification of the IDs 3 and 4 (*zp-sets*) and IDs 0–2 (*pp-sets*), see Table 1.

ID	File name	Number of jets
0	ascii_run_XY_pp_2tj_allhad_NLO_ptj1j2min200...	797 363
1	ascii_run_XY_pp_2tj_allhad_NLO_ptj1j2min60...	446 838
2	ascii_run_XY_pp_2tj_allhad_NLO_ptj1min200...	781 675
3	ascii_run_XY_zp_ttbarj_allhad_1000GeV..	449 606
4	ascii_run_XY_zp_ttbarj_allhad_1250GeV..	388 593

	ID	File name	Number of jets
→	0	data_zp	838 199
	1	data_pp	2 025 876

Table 1: Table of datasets generated using MadGraph5.

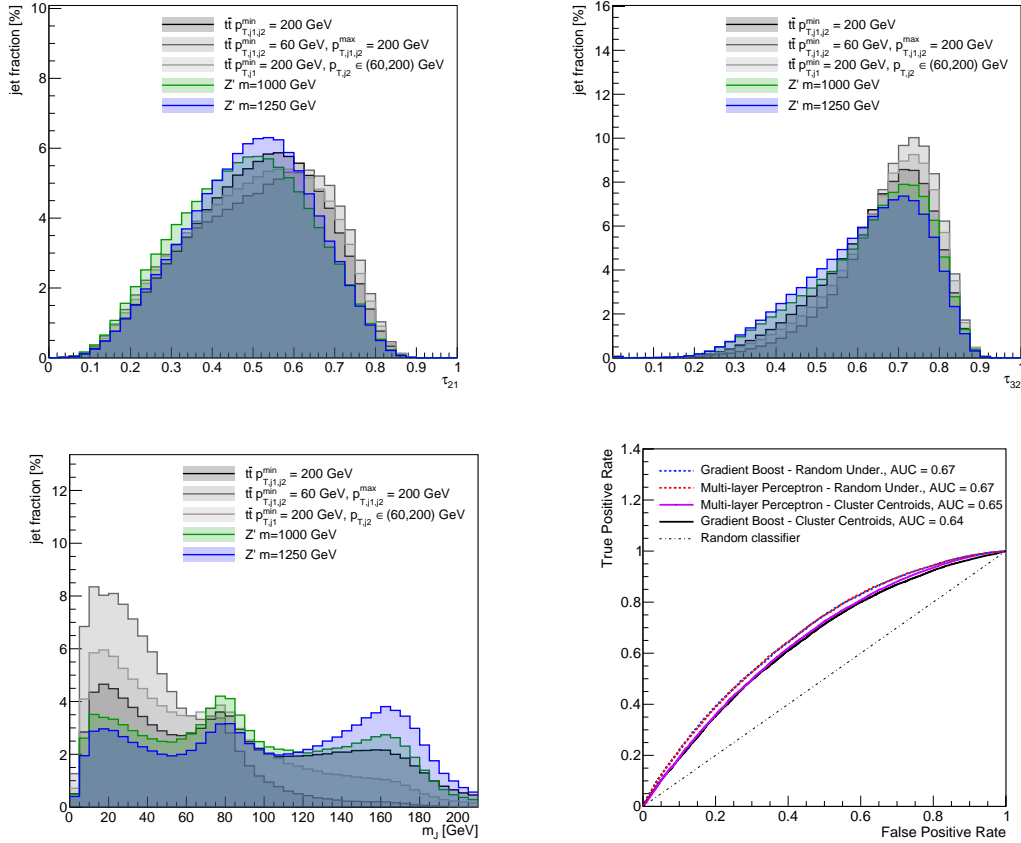


Figure 1: Shapes of the τ_{21} , τ_{32} subjettiness variables (top) and the large- R jet mass (bottom left) in the five samples used in training and testing of the tagging algorithms. Performance of top-tagging for different classifiers shown via ROC curve (bottom right).

The ratios between t-jets (W-jets) and light-jets are summarized in the following tables. Variables defined and used for each jet in the classification are as follows

Data set	t-jets	light-jets	Data set	W-jets	light-jets
data_zp_t	86%	14%	data_zp_w	48%	52%
data_pp_t	72.5%	27.5%	data_pp_w	42%	58%

Data set	t-jets	light-jets	Data set	W-jets	light-jets
data_zp_t	129 282	21 555	data_zp_w	110 735	121 658
data_pp_t	127 029	48 000	data_pp_w	180 169	251 422

Table 2: The ratios and number of jets of t-jets (W-jets) and light-jets.

event	$\Delta R(J,W)$	$\Delta R(J,t)$	p_T	η	ϕ	τ_{32}	τ_{21}	m	label
0	0.693589	0.280779	271.076000	-0.205725	1.034350	0.641589	0.304973	70.244600	l
0	1.152290	0.542026	161.364000	1.779510	-2.046550	0.678087	0.529191	67.632400	l
0	0.505954	0.876577	88.041000	0.431132	0.073586	0.468017	0.631805	7.432140	l
1	0.172936	0.046981	367.557000	-1.193480	-1.722920	0.840838	0.283345	75.302100	w
1	0.031584	0.143634	329.300000	-0.109191	1.337560	0.618819	0.205733	75.042200	w
2	0.143172	0.050171	501.473000	0.596318	-0.276567	0.605931	0.370552	171.372000	t

Table 3: Defined variables for each jet.

3 Jet Selection

The true type jets labels are then based on the following criteria

1. truth t-jets: $\Delta R(J, t) < 0.1 \wedge 138 \text{ GeV} \leq m_J \leq 208 \text{ GeV}$;
2. truth W-jets; $\Delta R(J, W) < 0.1 \wedge 60 \text{ GeV} \leq m_J \leq 100 \text{ GeV}$;
3. truth light jets: otherwise.

As a result, we have four subsets: zp-sets and pp-sets for t jets, and zp-sets and pp-sets for W jets Training sets contain 80% and the test sets 20% of data from the original sets.

4 Methods

In this section two approaches machine learning and cut-based are described in more detail.

4.1 Classifiers

- *Gradient boosting classifier* (GBC) - combining multiple simple predictors (here decision trees) to create a more powerful model

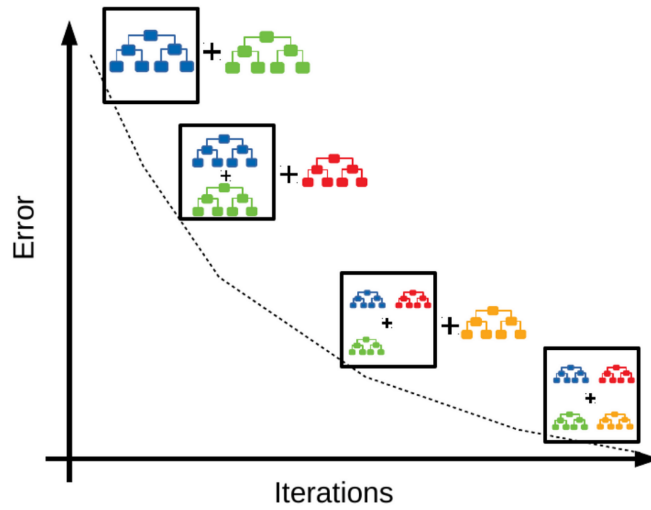


Figure 2: GBC

- *Multi-layer Perceptron classifier* (MLP) - based on neural networks.

4.1.1 Undersampling

- very distorted ratio between t-jets and light-jets (in the direction of t-jets)
- we settled for the undersampling applied to the training sets, which uses various techniques to remove data from the major class
- tested undersampling techniques: *Random undersampling*, *Cluster centroids*, *Near miss*, *Repeated edited nearest neighbor*

4.2 Cut-based algorithm

to identify jets coming from the hadronic decays of the W boson or a top quark by a simple cut-based algorithm

- W -jets if

$$0.10 < \tau_{21} < 0.60 \wedge 0.50 < \tau_{32} < 0.85 \wedge m_J \in [60, 100] \text{ GeV}$$
- top-jets if

$$0.30 < \tau_{21} < 0.70 \wedge 0.30 < \tau_{32} < 0.80 \wedge m_J \in [138, 208] \text{ GeV}$$

5 Results

5.1 Performance of algorithms

The ML-based method performance is shown in Figure 3 left, while cut-based method on the right.

We perform an exercise of finding a signal peak over a falling background by performing a background fit using a Bifurcated Gaussian function and an additional Gaussian function for the signal peak modelling. The signal significance calculated based on the fitted areas turns out to be slightly higher for cut-based method ($N_{\text{sig}}/\sqrt{N_{\text{bkg}}} \doteq 6.1$) compare to ML-based method ($N_{\text{sig}}/\sqrt{N_{\text{bkg}}} \doteq 5.6$). On the other hand the signal peak mass resolution (standard deviation of signal Gaussian fit) is smaller in case of the ML-based method, $\sigma \doteq 80$ GeV compare the the cut-based method, $\sigma \doteq 106$ GeV.

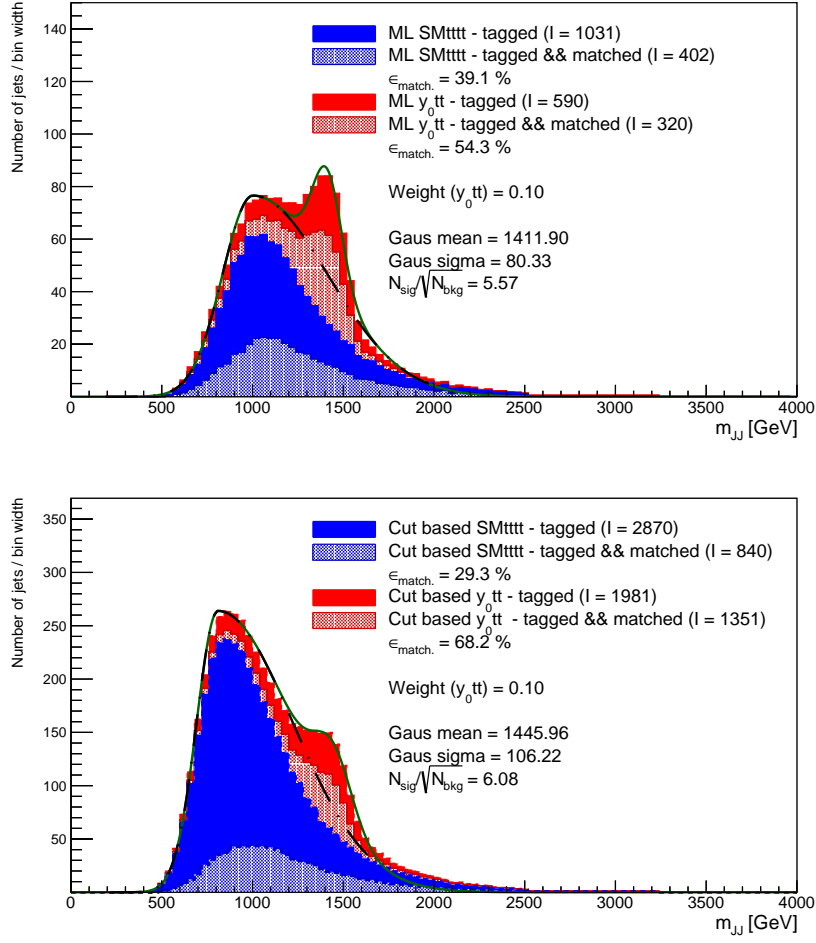


Figure 3: Invariant mass of two t -tagged jets (top ML based, bottom cut-based algorithm) for the process of SM $t\bar{t}t\bar{t}$ (blue area) representing background process with the stacked signal process $t\bar{t}y_0 \rightarrow t\bar{t}t\bar{t}$ (red area) scaled to its 10%. The light red and blue areas show tagged and matched jets to highlight the tagging efficiencies. The background fit is given by black line using Bifurcated Gaussian and green line is the Gaussian signal fit.

5.2 Comparison of best ML method and cut-based algorithm

In the Figure 4 we can see top tagging real efficiencies (red) and mistagging rates (blue) using cut-based (dashed lines) and ML-based (solid lines) of BSM $t\bar{t}y_0 \rightarrow t\bar{t}t\bar{t}$ as a function of jet mass (right). We can see that ML based algorithms give the same real efficiencies as cut-based, but significantly less fake efficiencies. Where real and fake efficiencies are defined as

$$\epsilon_{\text{real}} = \frac{N(\text{tagged \& matched})}{N(\text{tagged \& matched}) + N(\text{not - tagged \& matched})} \quad (1)$$

$$\epsilon_{\text{fake}} = \frac{N(\text{tagged \& not - matched})}{N(\text{tagged \& not - matched}) + N(\text{not - tagged \& not - matched})} \quad (2)$$

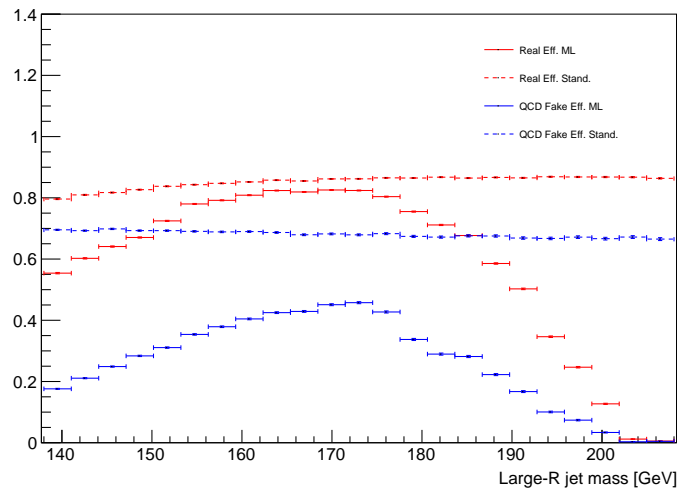


Figure 4: Efficiencies using cut-based and ML, $t\bar{t}y_0 \rightarrow t\bar{t}t\bar{t}$.

6 Conclusion

The real efficiencies of cut-based method in both t-jets and W -jets tagging are high about 80%, mostly flat, but unfortunately also having high mistagging rates about 65-70%. While ML-based method has lower efficiencies, the mistagging rates are suppressed compared to cut-based method.

Acknowledgements

The author would like to thank the grants of MSMT, Czech Republic, GAČR 23-07110S for the support.

References

- [1] Franz Gross et al. 50 Years of Quantum Chromodynamics. arXiv:2212.11107, December 2022. <https://arxiv.org/abs/2212.11107>.
- [2] Inderjeet Mani and Jianping Zhang. k-NN Approach to Unbalanced Data Distributions: A Case Study Involving Information Extraction. In *Proceedings of the Workshop on Learning from Imbalanced Datasets*, volume 126, 2003. <https://www.site.uottawa.ca/~nat/Workshop2003/jzhang.pdf>.
- [3] Hemashree Kilari. Gradient Boosting Classifier. Medium.com, 2023. <https://medium.com/@hemashreekilari9/understanding-gradient-boosting-632939b98764>.
- [4] Andreas G. Müller and Sarah Guido. *Introduction to Machine Learning with Python*. O'Reilly Media, Beijing, Boston, Farnham, Sebastopol, Tokyo, 2016. ISBN: 978-1-449-36975-8.
- [5] Jane Yen and Yue-Shi Lee. Cluster-Based Under-Sampling Approaches for Imbalanced Data Distributions. *Expert Systems with Applications*, 36(3):5718–5727, April 2009. <https://doi.org/10.1016/j.eswa.2008.06.108>.